Model for vortex pinning in a two-dimensional inhomogeneous *d*-wave superconductor

Daniel Valdez-Balderas* and David Stroud†
Department of Physics, The Ohio State University, Columbus, Ohio 43210, USA
(Received 1 August 2007; revised manuscript received 29 August 2007; published 11 October 2007)

We study a model for the pinning of vortices in a two-dimensional, inhomogeneous, type-II superconductor in its mixed state. The model is based on a Ginzburg-Landau (GL) free energy functional whose coefficients are determined by the mean-field transition temperature T_{c0} and the zero-temperature penetration depth $\lambda(0)$. We find that if (i) T_{c0} and $\lambda(0)$ are functions of position and (ii) $\lambda^2(0) \propto T_{c0}^{y}$ with $y > 0$, then vortices tend to be pinned by regions where T_{c0} and therefore the magnitude of the superconducting order parameter Δ are large. This behavior is in contrast to the usual picture of pinning in type-II superconductors, where pinning occurs in the small-gap regions. We also compute the local density of states of a model BCS Hamiltonian with *d*-wave symmetry, in which the pairing field Δ is obtained from the Monte Carlo simulations of a GL free energy. Several features observed in scanning tunneling spectroscopy measurements on $YBa_2Cu_3O_{6+x}$ and $Bi_2Sr_2CaCu_2O_{8+x}$ are well reproduced by our model: far from vortex cores, the local density of states spectra have a small gap and sharp coherence peaks, while near the vortex cores, they have a larger gap with low, broad peaks. Additionally, also in agreement with experiment, the spectra near the core do not exhibit a zero-energy peak which is, however, observed in other theoretical studies.

DOI: 10.1103/PhysRevB.76.144506 PACS number(s): 74.25.Qt, 74.81.−g, 74.25.Jb

I. INTRODUCTION

It is generally believed that vortices in type-II superconductors tend to be pinned in regions where the gap is small.[1] This is true because a vortex, being a region where the gradient of the superconducting order parameter is large, locally increases the gradient part of the free energy. Since this local increase is less in regions where the gap is smaller than average, the vortex tends to migrate to such regions, according to this picture.

In this paper, we describe a simple model for vortex pinning in an inhomogeneous two-dimensional (2D) superconductor, in which the vortices tend to be pinned in regions where the gap is *larger* than its spatial average. The model is based on a Ginzburg-Landau (GL) free energy functional in which both the mean-field transition temperature T_{c0} and the zero-temperature penetration depth $\lambda(0)$ are functions of position but are correlated in such a way that regions with large T_{c0} also have large $\lambda(0)$. This assumption seems to apply to some of the high-T_c cuprate superconductors: according to scanning tunneling microscopy (STM) experiments on cuprates,[2–9] regions that have a large gap (proportional to T_{c0} in this model) also have a single-particle local density of states (LDOS) with low, broad peaks, suggestive of a low superfluid density in these regions [proportional to $1/\lambda^2(0)$]. Our model is a generalization of an earlier approach intended to treat inhomogeneous superconductors in zero magnetic field.[10]

In order to further test this vortex pinning model, we also examine the quasiparticle LDOS near the vortex cores within this model. The proper theoretical description of this LDOS near the cores is one of the unsolved issues in the field of high-T_c superconductivity. STM experiments on $YBa_2Cu_3O_{6+x}$ (YBCO)[11,12] and $Bi_2Sr_2CaCu_2O_{8+x}$ (Bi2212),[13–16] show that the LDOS near vortex cores in those materials has the following characteristics: a dip at zero energy, small peaks at energies smaller than the superconducting gap, and low, broad peaks at energies above the superconducting gap. Those features contrast with the spectra shown by conventional superconductors near vortex cores, where the LDOS usually has a peak at zero energy in clean superconductors (i.e., those with a mean free path larger than the coherence length)[17,18] or is nearly energy independent in dirty superconductors.[18,19]

The zero-energy peak in the LDOS near vortex cores of clean conventional superconductors can be understood in terms of electronic states with subgap energies bound to vortex cores.[20,21] However, the structure of the spectra near vortex cores of cuprates is still lacking an explanation. Several authors have suggested that this structure is due to some type of competing order which emerges within the vortex cores when superconductivity is suppressed by a magnetic field.[22–26] Some of those models, and other descriptions of the spectra near vortex cores, have used the Bogoliubov–de Gennes method to solve various microscopic Hamiltonians,[22,27–31] such as BCS-like models with *d*-wave symmetry. One recent model for the LDOS near the vortex cores, proposed by Melikyan and Tesanovic,[30] used a Bogoliubov–de Gennes approach to a tight-binding Hamiltonian. These authors found that, if a homogeneous pairing field is used in the microscopic Hamiltonian, the LDOS exhibits a zero-energy peak on the atomic sites that are closest to the vortex cores; this peak is, however, absent from all other sites near the vortex cores. On the other hand, they found that introducing an enhanced pairing strength for electrons on nearest-neighbor atomic sites near the vortex cores leads to a suppression of the zero-energy peak, thus obtaining a better agreement with experiment. They speculate that the enhancement could be due to impurity atoms that pin the vortices, to a distortion of the atomic lattice by the vortex itself or to quantum fluctuations of the superconducting order parameter. The assumption of an enhanced pairing strength is consistent with the model that we describe in this paper.

In our model, having introduced this correlation between the GL parameters, we anneal the system to find both the

magnitude and the phase of the superconducting order parameter that minimize the GL free energy at low temperatures. Since the magnetic vector potential enters the GL free energy functional, this procedure naturally leads to vortex formation. The vortex cores can be identified in our simulations as regions with a large phase gradient. We find that, in inhomogeneous systems, vortices tend to be pinned in regions where the superconducting gap is large. For comparison, we also perform a similar annealing procedure for homogeneous systems. In this case, contrary to inhomogeneous systems, the magnitude of the superconducting order parameter is reduced near vortex cores. Thus, the assumption that the gap is large in regions with small superfluid density in inhomogeneous systems, originally intended to model superconductors in a zero magnetic field,[10] leads naturally to pinning of the vortices in large-gap regions. This approach might therefore be complementary to that of Ref. 30 mentioned above.

To connect our vortex pinning model to previous studies of the LDOS near vortex cores, we have also studied a microscopic Hamiltonian for electrons on a lattice. This is a tight-binding model in which electrons on nearest-neighbor sites experience a pairing interaction of the BCS type with d-wave symmetry.[10,32] The LDOS is obtained by exact numerical diagonalization of this Hamiltonian. We take the pairing strength between electrons on nearest-neighbor sites to be proportional to the value of the superconducting order parameter as determined by the GL simulations using the GL functional just described.

Using this combination of a GL free energy functional and a microscopic d-wave BCS Hamiltonian, we find that a number of experimental results on cuprates are reproduced well by our model for inhomogeneous systems. For example, far from vortex cores, the LDOS shows sharp coherence peaks. Near the vortex cores, our calculated LDOS does not show a spurious zero-energy peak; instead, it exhibits a large gap, as well as low, broad peaks which occur at energies larger than the value of the superconducting energy gap observed far from vortex cores. Also, in agreement with experiment, the LDOS curves near vortex cores are similar to those in the large-gap regions in systems with quenched disorder but *zero* magnetic field[10]; this connection is discussed in Sec. III. One feature not captured by our model is the existence of small, low energy peaks in the LDOS observed near the vortex cores.

The rest of the present paper is organized as follows. In Sec. II, we present the GL free energy functional, as well as the microscopic Hamiltonian. In Sec. III, we present results for homogeneous and inhomogeneous systems in a magnetic field, as well as results for inhomogeneous systems in a zero magnetic field for comparison. Finally, in Sec. IV, we conclude with a discussion and a summary of our work.

II. MODEL

A. Ginzburg-Landau free energy functional

We use a model for a single layer of a cuprate superconductor in a perpendicular magnetic field based on a GL free energy functional of the form described previously,[10]

$$\frac{F}{K_1} = \sum_{i=1}^{M} \left(\frac{t}{t_{c0i}} + 3 \right) \frac{1}{\lambda_i^2(0) t_{c0i}^2} |\psi_i|^2 + \sum_{i=1}^{M} \frac{1}{2(9.38)} \frac{1}{\lambda_i^2(0) t_{c0i}^4} |\psi_i|^4 - \sum_{\langle ij \rangle} \frac{2|\psi_i||\psi_j|}{\lambda_i(0) t_{c0i} \lambda_j(0) t_{c0j}} \cos(\theta_i - \theta_j + A_{\tilde{ij}}). \quad (1)$$

In Eq. (1), the first and second sums are carried over M square (XY) cells, each of whose area is equal to the zero-temperature GL coherence length squared ξ_0^2 of a square lattice into which the superconductor has been discretized for computational purposes. The third sum is carried out over nearest-neighbor cells $\langle ij \rangle$. Here,

$$\psi_i \equiv \frac{\Delta_i}{E_0}, \quad (2)$$

where Δ_i is the complex superconducting order parameter of the ith cell, E_0 is an arbitrary energy scale (which we take to be the hopping constant $t_{hop} \sim 200$ meV),

$$t \equiv \frac{k_B T}{E_0} \quad (3)$$

is the reduced temperature, T is the temperature, and k_B is the Boltzmann constant. Also, $\lambda_i(0)$ is the $T=0$ penetration depth and $t_{c0i} \equiv k_B T_{c0i}/E_0$, where T_{c0i} is the mean-field transition temperature of the ith cell. Therefore, in discretizing the superconductor, we have assumed that $\lambda(0)$, T_{c0}, and Δ are constant over distances of order ξ_0. Finally,

$$A_{\tilde{ij}} = \frac{2e}{\hbar c} \int_{\tilde{i}}^{\tilde{j}} \vec{A}(\vec{r}) \cdot d\vec{r} \quad (4)$$

is the integral of the vector potential $\vec{A}(\vec{r})$ from the center of cell i, located at $\vec{i}$, to the center of cell j, located at $\vec{j}$, and $K_1 \equiv \hbar^4 d/[32(9.38)\pi m^{*2} \mu_B^2]$, where $\mu_B^2 \simeq 5.4 \times 10^{-5}$ eV Å^3 is the square of the Bohr magneton, m^* is twice the mass of a free electron, e is the absolute value of its charge, and d is the thickness of the superconducting layer. In all of our simulations, we use periodic boundary conditions. A gauge for the magnetic field that allows this is given in Refs. 10 and 33 [see, e.g., Eq. (51) of Ref. 10, which gives this gauge choice explicitly].

We note that the connection between the local superfluid density $n_{s,i}(T)$ and penetration depth $\lambda_i(T)$ is such that $n_{s,i}(0) \propto 1/\lambda_i^2(0)$.[10] Thus, the quantity $1/\lambda^2$ in Eq. (1) is a way of describing the local superfluid density, which varies over a length scale of ξ_0.

We will be using the above free energy functional at both $T=0$ and finite T. Although we call this a "Ginzburg-Landau free energy functional," this name is really a misnomer since the original GL functional was intended to be applicable only near the mean-field transition temperature. Strictly speaking, the correct free energy functional near $T=0$ should not have the GL form but would be expected to contain additional terms, such as higher powers of $|\psi|^2$. We use the GL form for convenience, and because we expect that it will exhibit the qualitative behavior, such as vortex pinning in the large-gap regions, that would be seen in a more accurate functional.

We assume that the magnetic field is uniform, which is a good approximation for cuprate superconductors in their mixed state, provided that the external field is not too close to the lower critical field H_{c1}. In the cuprates, the approximation is satisfactory because the penetration depth is of the order of thousands of angstroms, while the intervortex distance for the fields we consider is ~100 Å. We employ a gauge that permits periodic boundary conditions, such that the flux through the lattice can take any integer multiple of hc/e.[10,33] Thus, the number N_v of flux quanta $hc/(2e)$ must be an integer multiple of 2.

The procedure for choosing the parameters $\lambda_i(0)$ and t_{c0i} is similar to that used in Ref. 10. Basically, in most of the system (α regions), we take $\lambda_i(0) \sim \lambda(0)$, where $\lambda(0)$ is the in-plane penetration depth of a bulk cuprate superconductor [$\lambda(0) \sim 1800$ Å in Bi2212, for example], while t_{c0i} is determined from the typical energy gap in the LDOS as observed in STM experiments. However, we will also introduce regions (β regions) in which t_{c0} and $\lambda(0)$ are larger than those bulk values. Throughout this paper, when we refer to a "gap in the LDOS," we mean the distance between the two peaks in the LDOS spectra. This is the same gap definition used in Ref. 4.

In Ref. 10, we generally introduced inhomogeneities in the superconducting order parameter Δ_i by assuming a binary distribution of t_{ci0}, randomly distributed in space: α cells with a small t_{ci0} and β cells with a large t_{ci0}. We also assumed a correlation between $\lambda_i(0)$ and t_{c0i} of the form

$$\lambda_i^2(0) = \lambda^2(0)\left(\frac{t_{c0i}}{t_{c0}}\right)^y, \tag{5}$$

with $y=1$. More generally, Eq. (5), with $y>0$, accounts for the fact that in STM experiments, regions with a large gap seem to have a small superfluid density (low and broad peaks.)

In the present paper, instead of randomly distributed β cells, we introduce two square regions with only β cells, while the rest of the lattice is assumed to have only α cells. We make this choice to study the effects of these inhomogeneities on field-induced vortices. We also consider a more general model than Ref. 10, allowing y to have values other than only $y=1$.

As shown in Eq. (36) of Ref. 10, in the absence of thermal fluctuations, the coupling constant $J_{XY,ij}$ between cells i and j is approximately

$$J_{XY,ij}(t) \simeq \frac{2(9.38)\sqrt{(1-t/t_{c0i})(1-t/t_{c0j})}}{\lambda_i(0)\lambda_j(0)}K_1. \tag{6}$$

(The factor of K_1 is missing in Ref. 10.) If $t \ll t_{c0i}$ and $t \ll t_{c0j}$, then

$$J_{XY,ij}(t) \simeq \frac{2(9.38)K_1}{\lambda_i(0)\lambda_j(0)}. \tag{7}$$

If we further choose a binary distribution of t_{c0i}, that is,

$$t_{c0i} = \begin{cases} t_{c0} & \text{if } i \text{ is on an } \alpha \text{ cell} \\ f t_{c0} & \text{if } i \text{ is on a } \beta \text{ cell,} \end{cases} \tag{8}$$

where f is any positive number (typically $f>1$), then

$$J_{XY,ij}(t) \simeq \frac{2(9.38)K_1}{\lambda^2(0)} \begin{cases} 1 & \text{if } i \text{ and } j \in \alpha \\ \dfrac{1}{f^{y/2}} & \text{if } i \in \alpha \text{ and } j \in \beta \text{ or if } i \in \beta \text{ and } j \in \alpha \\ \dfrac{1}{f^y} & \text{if } i \text{ and } j \in \beta. \end{cases} \tag{9}$$

This expression shows that in regions with a large gap, the coupling between XY cells is small, reflecting the large penetration depth in those regions.

B. Microscopic Hamiltonian

Besides using a GL free energy to explore vortex pinning in an inhomogeneous superconductor, we have also studied the LDOS of a corresponding microscopic model Hamiltonian, given by[10]

$$H = 2\sum_{\langle i,j\rangle,\sigma} t_{ij} c_{i\sigma}^\dagger c_{j\sigma} + 2\sum_{\langle i,j\rangle} (\Delta_{ij} c_{i\downarrow} c_{j\uparrow} + \text{c.c.}) - \mu \sum_{i,\sigma} c_{i\sigma}^\dagger c_{i\sigma}. \tag{10}$$

Here, $\Sigma_{\langle i,j\rangle}$ denotes a sum over distinct pairs of nearest-neighbor atomic sites on a square lattice with N sites, $c_{j\sigma}^\dagger$ creates an electron with spin σ ($\uparrow$ or $\downarrow$) at site j, μ is the chemical potential, and Δ_{ij} denotes the strength of the pairing interaction between electrons at sites i and j. Finally, we write t_{ij} as

$$t_{ij} = -t_{hop} e^{-iA'_{ij}}, \tag{11}$$

with

$$A'_{ij} = \frac{e}{\hbar c} \int_{\vec{i}}^{\vec{j}} \vec{A}(\vec{r}) \cdot d\vec{r}. \tag{12}$$

Here, the integral runs along the line from atomic site i, located at $\vec{i}$, to the atomic site j, located at $\vec{j}$, and $t_{hop} > 0$ is the hopping integral for nearest-neighbor sites on the lattice. Note that the prefactor in A'_{ij} involves the factor of hc/e due to a single electronic charge and is thus twice as large as that in A_{ij}, which involves the charge of a Cooper pair.

Following Ref. 10, we take Δ_{ij} to be given by

$$\Delta_{ij} = \frac{1}{4} \frac{|\Delta_i| + |\Delta_j|}{2} e^{i\theta_{ij}}, \tag{13}$$

where

$$\theta_{ij} = \begin{cases} (\theta_i + \theta_j)/2 & \text{if bond } \langle i,j \rangle \text{ is in the } x \text{ direction} \\ (\theta_i + \theta_j)/2 + \pi & \text{if bond } \langle i,j \rangle \text{ is in the } y \text{ direction,} \end{cases} \tag{14}$$

and

$$\Delta_j = |\Delta_j| e^{i\theta_j} \tag{15}$$

is the value of the complex superconducting order parameter at site j. We will refer to the lattice over which the sums in Eq. (10) are carried out as the *atomic* lattice (in order to distinguish it from the XY lattice.) The first term in Eq. (10) thus corresponds to the kinetic energy, the second term is a BCS type of pairing interaction with d-wave symmetry, and the third is the energy associated with the chemical potential.

The model we present is similar to the one presented in Ref. 10, the main differences being the inclusion of a vector potential in the GL free energy functional and the spatial distribution of the inhomogeneities. Because the vector potential introduces vortices in the system, our results differ substantially from our previous work.

III. RESULTS

We first present results for homogeneous systems in the presence of an applied transverse magnetic field equal to two flux quanta through the lattice at low T. This is the lowest magnetic field consistent with the periodic boundary conditions. In this case, t_{c0i} and $\lambda_i(0)$ are independent of i. Figure 1 shows our calculated maps of Δ for a homogeneous system. In part (a), the lengths and directions of the arrows represent the magnitude and phase of Δ in each XY cell. Even though t_{c0i} is homogeneous, the magnetic field renders Δ inhomogeneous, especially near the vortex cores, where Δ has a large phase gradient and a smaller magnitude. This behavior is familiar from Ginzburg-Landau treatments of homogeneous type-II superconductors in a magnetic field. Part (b) of Fig. 1 shows a map of $|\Delta|$, with dark (light) regions representing small (large) value of $|\Delta|$. The vortex cores are the darkest regions.

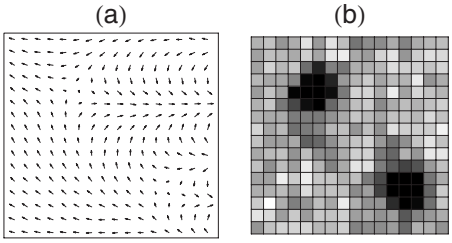

FIG. 1. Map of the pairing field Δ over a homogeneous, two-dimensional superconductor of area $16\xi_0 \times 16\xi_0$ in a transverse, uniform magnetic field $B \simeq 6$ T. The superconductor has been discretized into XY cells, each of which has an area ξ_0^2 and encloses nine atomic sites. In part (a), the length and direction of each arrow represent the complex value of Δ within an XY cell. Part (b) shows a map of the magnitude $|\Delta|$ of the pairing field. Dark (light) regions represent a small (large) value of $|\Delta|$. Vortex cores can be easily identified as the darkest regions.

Figure 2 show the LDOS averaged over regions near and far from the vortex cores of the system described in Fig. 1. Since $|\Delta|$ is small near the core, we have defined an XY cell to be "near the core" if $|\Delta| \leq |\Delta_{av}|/2$ in that cell, where $|\Delta_{av}|$ is the value of $|\Delta|$ averaged over all the XY cells of the lattice. All other cells are considered to be far from the core. Thus, in order to compute the averaged quantities shown in Fig. 2, we first calculated the LDOS on every atomic site by exact numerical diagonalization of the Hamiltonian [Eq. (10)] and then averaged the LDOS over the set of atomic sites near and far from the vortex cores, as defined above. We have chosen to enclose nine atomic sites inside each XY cell for this system because the coherence length in cuprates is ~ 15 Å, approximately three times larger than the atomic lattice constant, ~ 5 Å.

Figure 2 shows that, in a homogeneous system, the LDOS far from the core is strongly suppressed near $\omega = 0$ and exhibits sharp coherence peaks, reminiscent of a d-wave superconductor in the absence of a magnetic field. Near the vortex cores, on the other hand, the gap is filled, and the LDOS is large near $\omega = 0$, resembling the spectrum of a gapless tight-

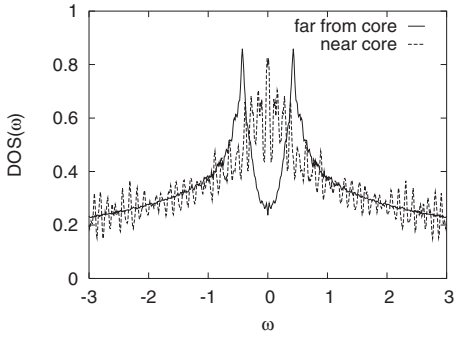

FIG. 2. Local density of states averaged over two different groups of XY cells in the homogeneous superconductor described in Fig. 1: far from the vortex core (full curve) and near the core (dotted curve). The oscillations in the dotted curve are due to numerical fluctuations arising from the small number of sites in the core regions.

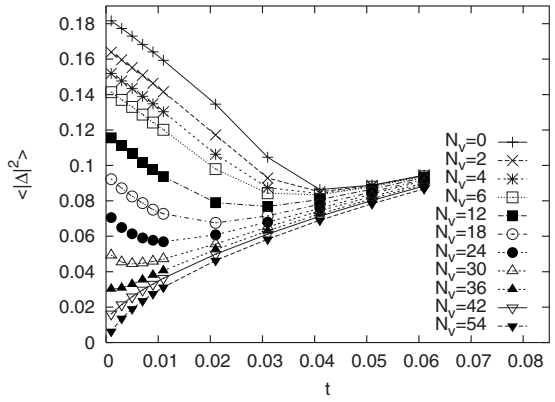

FIG. 3. Thermal average $\langle|\Delta|^2\rangle$ of the squared magnitude of the superconducting order parameter versus the reduced temperature t for a system with a homogeneous t_{c0} placed in various fields. The magnitude of the magnetic field is $B \simeq N_v \times 3$ T as described in the text. We can observe that the minimum of $\langle|\Delta|^2\rangle$ (t) versus t [which is known to occur near the phase ordering temperature in zero magnetic field systems (Refs. 10 and 37)] is shifted toward smaller values of t with increasing magnetic field.

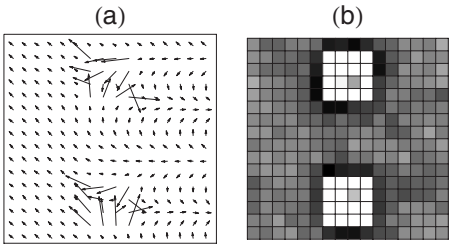

FIG. 4. Map of the pairing field Δ in an inhomogeneous, two-dimensional superconductor of area $16\xi_0 \times 16\xi_0$ in a transverse, uniform magnetic field $B \simeq 6$ T. The superconductor has two β regions where t_{c0i} is large; these correspond to the light regions in (b). The system has been discretized into XY cells, each of which has an area ξ_0^2 and encloses nine atomic sites. In part (a), each arrow represents the complex value of Δ within an XY cell. Part (b) shows a map of the magnitude $|\Delta|$ of the pairing field. Dark (light) regions represent a small (large) value of $|\Delta|$. The locations of the two vortex cores can be identified as the regions with a large phase gradient in part (a). They are pinned to regions with a large $|\Delta|$ because of the low value of the coupling between XY cells in those regions. The present results are obtained from Eqs. (8) and (9), using $f=3$ and $y=3$.

binding model in two dimensions and zero magnetic field.[10,34] The spectrum near the core has considerable numerical noise because it represents an average over only a few atomic sites. In particular, the rapid oscillations are probably due to this numerical artifact.

To estimate our magnetic fields, we note that, because of the numerical implementation of the periodic boundary conditions,[10,35] the field has to be chosen so that the number N_v of magnetic flux quanta $\Phi_0 = hc/(2e)$ through the system is a multiple of 2. Therefore, the magnetic field can be estimated using $B = N_v \Phi_0 / S$, where S is the area of the system and $\Phi_0 \equiv hc/(2e) \approx 2 \times 10^{-15}$ T m^2. In the present paper, we use a numerical sample of area $S = (48a_0)^2$, where $a_0 \sim 5$ Å is the atomic lattice constant. Therefore, $B \approx N_v \times 3$ T, and for the systems containing two vortices, $B \sim 6$ T. The magnitude of this magnetic field is comparable to that used in STM experiments.[13,14]

We now briefly discuss the temperature evolution of $\langle|\Delta|^2\rangle$, defined as an average of $\langle|\Delta_i|^2\rangle$ over all XY lattice cells i, for systems with homogeneous t_{c0} in a transverse magnetic field. Here, $\langle\cdots\rangle$ denotes a thermal average, obtained using Monte Carlo simulations. Figure 3 shows curves of $\langle|\Delta|^2\rangle(t)$ versus reduced temperature t, for systems of the same size subject to different magnetic fields and therefore containing different numbers of vortices N_v. In the zero magnetic field case, $N_v = 0$, $\langle|\Delta|^2\rangle(t)$ has a minimum as a function of t, which occurs near the phase ordering temperature. Figure 3 shows that, as the field is increased, the phase ordering temperature is reduced, and around $N_v = 36$, it seems to drop to zero. The fact that $\langle|\Delta|^2\rangle(t)$ increases with t for large t is an artifact of the GL functional, as has been discussed in detail in Ref. 10 for the case $B=0$.

We now proceed to show systems with inhomogeneities. Figure 4 shows gap maps of systems in which t_{c0i} and therefore $J_{XY,ij}$ are i dependent. Specifically, two square regions, of size 4×4 XY cells each, have $t_{c0i} = f t_{c0}$, with $f=3$; those are called β cells, as described in the previous section. The remainder of the XY cells have $t_{c0i} = t_{c0}$ and are called α cells. Clearly, the vortices are pinned in the β regions, where $|\Delta|$ is large. The fact that $|\Delta|$ is large in β regions is of course due to the fact that at low temperatures, $|\Delta|$ is roughly proportional to t_{c0}. On the other hand, in order to understand why the vortices are pinned in the large-$|\Delta|$ regions, we note that $J_{XY,ij}$ at low temperatures can be estimated with the use of Eq. (9). For the particular parameters used in this calculation, namely, $y=3$ and $f=3$, $J_{XY,ij}$ is about 27 times smaller within β regions than in the α regions. Because of this ratio, phase gradients near the vortex cores cost much less energy in the β regions than in the α regions, even though $|\Delta|$ is larger in the β regions. Thus, it is energetically favorable for the vortices to be pinned in the β regions.

Figure 5 shows the LDOS averaged over α and β regions of the system shown in Fig. 4. This figure shows that, far from the vortex cores (α regions), the LDOS is very similar to that of regions far from the core in the homogeneous system at low magnetic field (cf. Fig. 2)—both spectra have a small gap and sharp coherence peaks. However, in contrast to the homogeneous case, the LDOS of the inhomogeneous system exhibits a large gap and broadened peaks near the vortex core. This LDOS spectrum is similar to that calculated for the large-gap regions of systems with quenched disorder and no magnetic field in our previous work.[10] In the present case, the gap in the LDOS is large in the β regions, of course, because of the large value of t_{c0i} and therefore of $|\Delta|$, near the vortex cores. The peaks in the LDOS in the β region above the gap are low and broad, on the other hand, because of the large phase gradient of the superconducting order parameter in these regions. It is as if the system has lost phase coherence in those regions due to the presence of the vortex core. We can more clearly see this point by comparing the LDOS of a β region containing a pinned vortex core to that of a β region in a system in a zero magnetic field, in which,

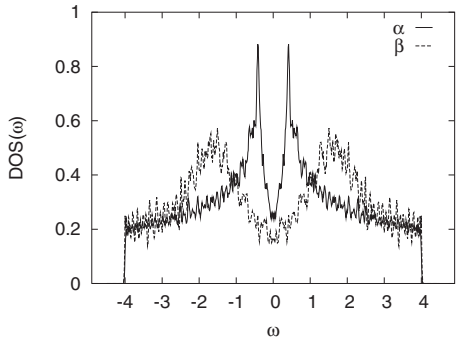

FIG. 5. Local density of states averaged over two different groups of *XY* cells in the inhomogeneous superconductor shown in Fig. 4: far from the core (α) and near the core (β). In agreement with experimental results, this figure shows that (i) far from vortex cores, the LDOS shows sharp coherence peaks, and (ii) near the vortex cores, the LDOS does not display the unphysical zero-energy peak obtained in other models. Instead (iii), it has a large gap, as well as low and broad peaks.

therefore, there is no vortex core to be pinned. We now describe this system.

Figure 6 shows a system at low temperature with two inhomogeneities, similar to that shown in Fig. 4, but with zero rather than a finite magnetic field. Clearly, in the ground state, as expected, the phase of Δ is almost uniform. Furthermore, and also as expected, $|\Delta|$ is larger in the β regions, which have a larger value of t_{c0i}. However, when we turn to the LDOS (Fig. 7), the LDOS of the β regions is characterized by much sharper coherence peaks than that at finite magnetic field described in the previous paragraph, presumably because of the absence of a large phase gradient.

We have also tested the sensitivity of our results to the lattice size and to the number of atomic sites per *XY* cell. To do this, we performed calculations similar to the ones described above, but with 24×24 instead of 16×16 *XY* lattices, each *XY* cell containing four instead of nine atomic lattice sites. Figure 8 shows the results for a 24×24 *XY* lattice of an inhomogeneous system in the presence of a magnetic field. As in the 16×16 case, the vortices are pinned in the regions with large Δ and small $J_{XY,ij}$. Figure 9 shows that the LDOS for this system both near and far from the core is nearly the same as that of the 16×16 system shown

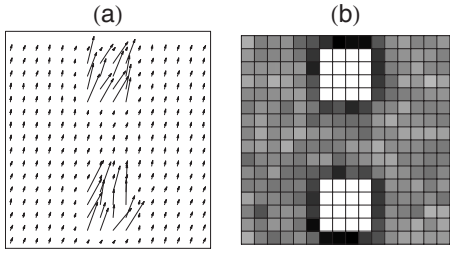

FIG. 6. Same as Fig. 4, but for a system at $B=0$ instead of $B\neq0$. At low temperatures, the phase of Δ is almost uniform since, in the absence of a magnetic field, phase gradients cost energy. As expected, Δ is larger in the β regions, which have a large value of t_{c0i}.

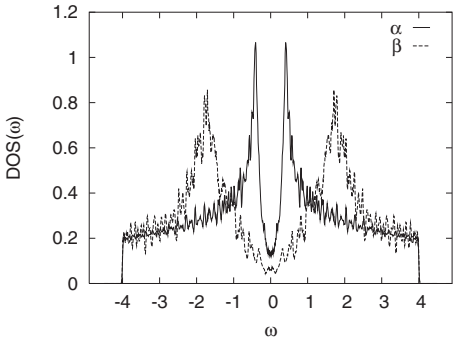

FIG. 7. Local density of states for the system shown in Fig. 6. The LDOS in the β regions of this system has much sharper peaks than the LDOS of the β regions for the corresponding system in a finite magnetic field shown in Fig. 5. This result shows that having a large gap is not a sufficient condition to observe broadened peaks near vortex cores; a large phase gradient is also required.

in Fig. 5. Likewise, a system with 24×24 *XY* cells and two atomic sites per *XY* cell, but with no magnetic field, is shown in Fig. 10; the corresponding LDOS averaged over regions near and far from the core is shown in Fig. 11. The LDOS shown in this figure has the same features as that of the 16×16 system shown in Fig. 7. We thus conclude that our results are not very sensitive to the lattice sizes used nor to the number of atomic sites per *XY* cell.

In the calculations described above, we have assumed that $\lambda^2\propto T_{c0}^y$. If $y\geq3$, then the vortices are consistently pinned in the large-gap region. By contrast, if $y=1$, we find that the vortices may or may not be pinned in the large-gap region, depending on where these regions are located within the computational lattice. The vortices obviously go to the large-gap region because of the correlation between λ^2 and T_{c0}. As mentioned earlier, this correlation originates in the fact that large λ^2 implies a small energy cost to introduce a gradient in the phase of the order parameter. Such a gradient must exist near a vortex core; therefore, the vortex prefers to be in a region where this gradient is energetically inexpensive. Melikyan and Tesanovic[30] discuss various other possible causes of larger pinning in the large-gap region; these include quantum fluctuations, distortion of the atomic lattice by the vortices, and the pinning of vortices by impurity atoms. Our model could be viewed as a special kind of such impurity pinning, in which the "impurities" are superconducting regions with a large gap and large penetration depth. We have also looked at how the size of the pinning regions affects the

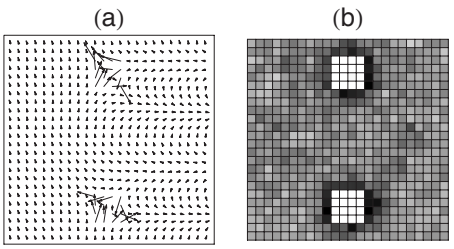

FIG. 8. Similar to Fig. 4, but the system has 24×24 instead of 16×16 *XY* cells, each with four instead of nine atomic lattice sites.

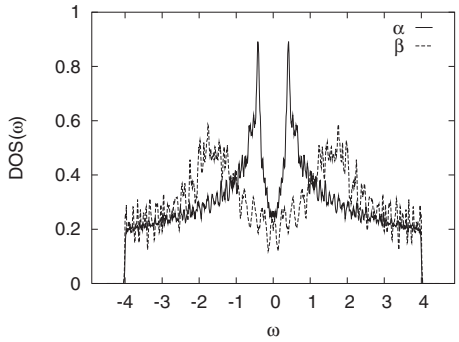

FIG. 9. Local density of states averaged over regions far from the vortex cores, for the system shown Fig. 8. Results are very similar to the corresponding system with 16×16 cells, which has nine instead of four atoms per *XY* cell and is shown in Fig. 5. Thus, our results are not strongly dependent on the size of the *XY* cell or of the *XY* lattice.

pinning. The pinning is generally more effective for large pinning regions, probably because the vortex energy is reduced by a larger amount if pinned in a region of large pinning area, all other parameters being the same.

Finally, we note the similarity between our calculated LDOS versus energy curves for regions near the vortex cores and the corresponding curves for large-gap regions of inhomogeneous systems with quenched disorder in a zero magnetic field, calculated in our previous work.[10] Those similarities have been implied in several experimental papers. For example, Lang *et al.*[4] discussed the similarity between the spectra of large-gap regions of inhomogeneous systems at low temperatures in a zero field and those observed in the pseudogap regime of some cuprate superconductors. In the pseudogap region, the phase configuration is disordered and therefore, possibly like the β region at zero field, both might be considered as "normal" regions. Likewise, Fischer *et al.*[36] have also noted the similarity of the low-T spectra near the vortex cores to spectra in the pseudogap regime. Once again, the similarity may arise because both the interior of the vortex cores and the pseudogap region may be considered as normal. Thus, both of these reports implicitly suggest a similarity between the low-T spectra in the large-gap regions of a disordered system at $B=0$ and the corresponding spectra near vortex cores at finite B.

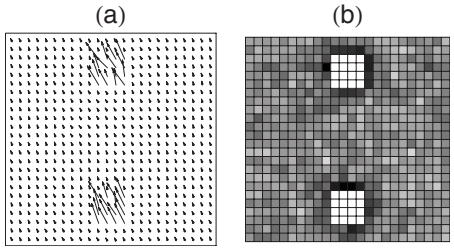

FIG. 10. Same as Fig. 6 but for a system consisting of 24×24 instead of 16×16 *XY* cells, each having four instead of nine atomic sites.

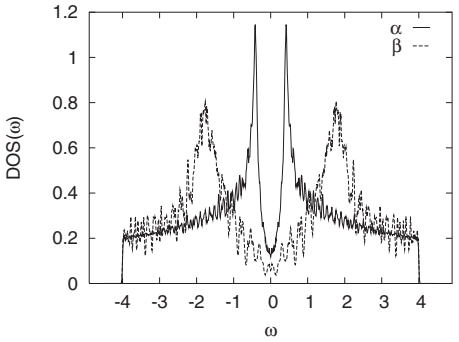

FIG. 11. Same as Fig. 7 but for a system of 24×24 instead of 16×16 *XY* cells, each having four rather than the nine atomic sites.

IV. DISCUSSION

We have presented a model for the pinning of vortices by inhomogeneities in a two-dimensional type-II superconductor at low temperatures. The model is based on a GL free energy functional, and it is inspired by our previous study[10] of the LDOS in an inhomogeneous superconductor in zero magnetic field. In our model, we have proposed a GL free energy functional in which regions with a large value of the superconducting order parameter have a large penetration depth, as suggested by zero-field STM experiments on cuprates. Using an annealing process and Monte Carlo simulations, we have found that the pinning of vortices by those large-gap regions emerges naturally from the functional form of our GL free energy. The vortices are attracted to the large-gap regions, in our model, because the large penetration depth leads to a small coupling between cells in those regions. Therefore, the phase of the superconducting order parameter can more easily bend in these regions, and this in turn allows the large-gap regions to accommodate a vortex more easily than regions with a small gap. By contrast, in the absence of quenched inhomogeneities, minimization of the GL free energy functional yields a spatial configuration in which the superconducting order parameter is suppressed near vortex cores.

It is worth commenting further on the qualitative physics underlying the pinning of the vortices in the region of enhanced local T_{c0}. Basically, this pinning behavior occurs because, in our model, a locally enhanced T_{c0} corresponds to a locally suppressed superfluid density. This superfluid density is proportional to the local $1/\lambda^2$ and is related to the Ginzburg-Landau coefficients, as we have described earlier. The vortices can be more easily accommodated in these large-T_{c0} regions because the large phase gradients which characterize the vortices cost less energy in such regions. Although we describe the pinning in terms of the variation of $1/\lambda^2$, the pinning is not due to any kind of "magnetic" forces—the quantity $1/\lambda^2$ is just a way of describing the local superfluid density. Thus, just as in conventional pinning, the vortices are attracted to regions of lower free energy. The major difference is that the superfluid density (and $1/\lambda^2$) is inversely proportional to T_{c0} in the present model, rather than being independent of or directly correlated with T_{c0} as in more conventional pinning. This leads to pinning in

a large-T_{c0} region rather than a small-T_{c0} region. We also emphasize that, although our pinning results are obtained using rather elaborate numerical calculations, the underlying physics is straightforward: the pinning behavior is consistent with qualitative expectations, given the model.

It may seem strange to consider the spatial variation in $1/\lambda^2$ as occurring over a scale of $\xi_0 \sim 15$ Å, when λ itself is of order 10^3 Å or more. However, it should be remembered that $1/\lambda^2$ is related to the coefficients of the Ginzburg-Landau free energy [see Eq. (1)], and these coefficients are, in fact, expected to vary over a scale of ξ_0. Thus, the model is, indeed, reasonable and consistent with the expected physics. It is the local superfluid density (proportional to $1/\lambda^2$) which varies over a scale of ξ_0.

It is also worth commenting on what kind of real systems could be described by our model. Even if one neglects the weak Josephson coupling between the layers of a high-T_c material, there will still be magnetic interactions between pancake vortices in adjacent layers, so that the system will not be truly 2D. Likewise, if we wish to use this model to describe a very thin 2D high-T_c film, there are stray fields in vacuum extending into the third dimension, which will contribute to the total energy. In both cases, our model is definitely an oversimplification. Nonetheless, our model does seem to describe some observed features in real high-T_c materials, suggesting that it captures some significant physics in these systems. Thus, we consider our model as a possible starting point for a fully realistic treatment of either three-dimensional high-T_c materials or very thin 2D high-T_c layers.

We have connected our work on the pinning of vortices to continuing efforts by several groups to describe the density of states near vortices in cuprate superconductors. To do this, we have studied a model BCS Hamiltonian with *d*-wave symmetry, in which the pairing field is obtained from simulations of the GL free energy functional. We use exact diagonalization to compute the local density of states on each atomic site of the lattice described by this Hamiltonian. For homogeneous systems, we found that the LDOS near the vortex cores resembles that of a gapless tight-binding model in two dimensions, with a Van Hove peak at zero energy. However, when we introduce the inhomogeneities with a large pairing field and large penetration depth that pin the vortices, the LDOS near the vortex cores is markedly different from that of the homogeneous systems. Namely, this LDOS exhibits a large gap as well as low and broadened peaks at energies greater than that of the superconducting gap far from the vortex core. Also, our calculated LDOS near the vortex cores in this inhomogeneous case does not exhibit the spurious zero-energy peak, which is present in several other theoretical studies but is absent from experiments. All of these features in our calculations are consistent with results observed in STM experiments on YBCO[11,12] and Bi2212.[13–16]

Our results are also consistent with those obtained in Ref. 30, using a somewhat different model. Those authors obtain better agreement between their calculated LDOS spectra and experiment,[14] if they assume an enhanced rather than uniform pairing field near the vortex cores. In particular, introducing this large pairing field near the vortex core in their model suppresses the unphysical zero-energy peak. Our approach, in which a large gap is correlated with a large penetration depth, may help justify the occurrence of this larger pairing field in the vortex cores.

Finally, we briefly comment on the possible physical origin of correlation between large gap and large penetration depth. The origin of the spatial fluctuations of T_{c0} observed in the cuprates may be the local fluctuations in concentration of charge carriers, which are highly likely since the cuprates are mostly disordered alloys and the local concentration would involve an average coherence length, which is only about 15 Å. However, T_{c0} is proportional to the gap (i.e., presumably, the pseudogap), which increases with decreasing concentration of charge carriers, whereas $1/\lambda^2(0)$ is proportional to the superfluid density, which should decrease with decreasing charge carrier concentration. Therefore, we expect T_{c0} to be positively correlated with $\lambda^2(0)$, as seen experimentally and as used in the present model.

ACKNOWLEDGMENTS

This work was supported by NSF Grant No. DMR04-13395. The computations described here were carried out through a grant of computing time from the Ohio Supercomputer Center. We thank J. Orenstein for a useful conversation about the origin of the correlation between superconducting gap and penetration depth.

*valdez@pas.rochester.edu
†stroud@mps.ohio-state.edu

[1] G. Blatter, M. V. Feigel'man, V. B. Geshkenbein, A. I. Larkin, and V. M. Vinokur, Rev. Mod. Phys. **66**, 1125 (1994).
[2] T. Cren, D. Roditchev, W. Sacks, J. Klein, J.-B. Moussy, C. Deville-Cavellin, and M. Lagues, Phys. Rev. Lett. **84**, 147 (2000).
[3] C. Howald, P. Fournier, and A. Kapitulnik, Phys. Rev. B **64**, 100504(R) (2001).
[4] K. M. Lang, V. Madhavan, J. E. Hoffman, E. W. Hudson, H. Eisaki, S. Uchida, and J. C. Davis, Nature (London) **415**, 412 (2002).
[5] C. Howald, H. Eisaki, N. Kaneko, M. Greven, and A. Kapitulnik, Phys. Rev. B **67**, 014533 (2003).
[6] T. Kato, S. Okitsu, and H. Sakata, Phys. Rev. B **72**, 144518 (2005).
[7] A. C. Fang, L. Capriotti, D. J. Scalapino, S. A. Kivelson, N. Kaneko, M. Greven, and A. Kapitulnik, Phys. Rev. Lett. **96**, 017007 (2006).
[8] H. Mashima, N. Fukuo, Y. Matsumoto, G. Kinoda, T. Kondo, H. Ikuta, T. Hitosugi, and T. Hasegawa, Phys. Rev. B **73**, 060502(R) (2006).
[9] S. H. Pan *et al.*, Nature (London) **413**, 282 (2001).
[10] D. Valdez-Balderas and D. Stroud, Phys. Rev. B **74**, 174506

(2006).
[11] I. Maggio-Aprile, C. Renner, A. Erb, E. Walker, and O. Fischer, Phys. Rev. Lett. **75**, 2754 (1995).
[12] C. Renner, B. Revaz, K. Kadowaki, I. Maggio-Aprile, and O. Fischer, Phys. Rev. Lett. **80**, 3606 (1998).
[13] G. Levy, M. Kugler, A. A. Manuel, O. Fischer, and M. Li, Phys. Rev. Lett. **95**, 257005 (2005).
[14] S. H. Pan, E. W. Hudson, A. K. Gupta, K.-W. Ng, H. Eisaki, S. Uchida, and J. C. Davis, Phys. Rev. Lett. **85**, 1536 (2000).
[15] K. Matsuba, H. Sakata, N. Kosugi, H. Nishimori, and N. Nishida, J. Phys. Soc. Jpn. **72**, 2153 (2003).
[16] B. Hoogenboom, C. Renner, B. Revaz, I. Maggio-Aprile, and O. Fischer, Physica C **332**, 440 (2000).
[17] H. F. Hess, R. B. Robinson, and J. V. Waszczak, Phys. Rev. Lett. **64**, 2711 (1990).
[18] C. Renner, A. D. Kent, P. Niedermann, O. Fischer, and F. Lévy, Phys. Rev. Lett. **67**, 1650 (1991).
[19] Y. De Wilde, M. Iavarone, U. Welp, V. Metlushko, A. E. Koshelev, I. Aranson, G. W. Crabtree, and P. C. Canfield, Phys. Rev. Lett. **78**, 4273 (1997).
[20] C. Caroli, P. G. D. Gennes, and J. Matricon, Phys. Lett. **9**, 307 (1964).
[21] J. D. Shore, M. Huang, A. T. Dorsey, and J. P. Sethna, Phys. Rev. Lett. **62**, 3089 (1989).
[22] M. Franz and Z. Tesanovic, Phys. Rev. Lett. **80**, 4763 (1998).
[23] D. P. Arovas, A. J. Berlinsky, C. Kallin, and S.-C. Zhang, Phys. Rev. Lett. **79**, 2871 (1997).
[24] M. Franz and Z. Tesanovic, Phys. Rev. B **63**, 064516 (2001).
[25] J. H. Han and D.-H. Lee, Phys. Rev. Lett. **85**, 1100 (2000).
[26] J.-i. Kishine, P. A. Lee, and X.-G. Wen, Phys. Rev. B **65**, 064526 (2002).
[27] P. I. Soininen, C. Kallin, and A. J. Berlinsky, Phys. Rev. B **50**, 13883 (1994).
[28] Y. Wang and A. H. MacDonald, Phys. Rev. B **52**, R3876 (1995).
[29] J.-X. Zhu and C. S. Ting, Phys. Rev. Lett. **87**, 147002 (2001).
[30] A. Melikyan and Z. Tesanovic, Phys. Rev. B **74**, 144501 (2006).
[31] O. Vafek, A. Melikyan, M. Franz, and Z. Tesanovic, Phys. Rev. B **63**, 134509 (2001).
[32] T. Eckl, D. J. Scalapino, E. Arrigoni, and W. Hanke, Phys. Rev. B **66**, 140510(R) (2002).
[33] W. Yu, K. H. Lee, and D. Stroud, Phys. Rev. B **47**, 5906 (1993).
[34] F. F. Assaad, Phys. Rev. B **65**, 115104 (2002).
[35] W. Yu, K. H. Lee, and D. Stroud, Phys. Rev. B **47**, 5906 (1993).
[36] O. Fischer, M. Kugler, I. Maggio-Aprile, C. Berthod, and C. Renner, Rev. Mod. Phys. **79**, 353 (2007).
[37] E. Bittner and W. Janke, Phys. Rev. Lett. **89**, 130201 (2002).